Available online at www.sciencedirect.com
SCIENCE DIRECT
Journal of Catalysis 240 (2006) 31–38
JOURNAL OF CATALYSIS
www.elsevier.com/locate/jcat

Role of surface pockets on MCM-49 structure in the alkylation of hydroquinone with *tert*-butanol

Bingjun Xu [a], Huiyun Li [b], Weiming Hua [a], Yinghong Yue [a,*], Zi Gao [a,*]

[a] *Department of Chemistry and Shanghai Key Laboratory of Molecular Catalysis and Innovative Materials, Fudan University, Shanghai 200433, PR China*
[b] *Department of Chemistry, Anyang Teachers College, Henan, Anyang 455002, PR China*

Received 16 December 2005; revised 20 February 2006; accepted 26 February 2006

Available online 3 April 2006

Abstract

A series of MCM-49 catalysts with different Si/Al ratios were prepared and characterized by XRD, XRF, ^{27}Al MAS NMR, BET, and SEM. The overall and external surface acidity of the catalysts were measured by temperature-programmed desorption of both small- and large-base probe molecules (NH_3 and 2,6-di-*tert*-butyl-pyridine), as well as by model acid-catalyzed reactions, such as cumene cracking and 1,3,5-tri-*tert*-butylbenzene dealkylation, and compared with those of ZSM-5 and USY zeolites. The strong external acid sites on the surface pockets of MCM-49 play an important role in the alkylation of hydroquinone with *tert*-butanol. MCM-49 catalyst with a Si/Al ratio of 20 exhibits good activity and selectivity for the alkylation reaction, and it is more reusable than mesoporous molecular sieves such as AlSBA-15 and MSU-$S_{(BEA)}$ due to the higher thermal and hydrothermal stability of the crystalline zeolite framework.

Keywords: MCM-49; Alkylation; 2-*tert*-Butyl-hydroquinone; External surface acidity; Reusability

1. Introduction

Alkylation of hydroquinone with *tert*-butanol to synthesize 2-*tert*-butyl-hydroquinone (2-TBHQ) is an interesting reaction, because 2-TBHQ is an excellent antioxidant widely used in the food industry as well as a good stabilizer in the plastics and rubber industries [1]. It is a typical acid-catalyzed Friedel–Crafts reaction conventionally using liquid mineral acids (e.g., phosphoric acid and sulfuric acid) as catalysts [2,3]. As awareness of the importance of environmental protection grows, finding alternatives to non-reusable and pollution-causing liquid acid catalysts is highly desirable.

Various solid acid catalysts have been tried in the alkylation of hydroquinone, phenols, and anisole with *tert*-butanol, including silica gel [4], ion-exchanged layered tetra silicic mica [5], Amberlyst-15 [6], and various K-10 clay-supported catalysts [7–10]. Mesoporous materials, such as a combination of HMS and sulfated zirconia [11], MCM-41, and MCM-48 [12,13], have also been used as catalysts in this kind of reaction.

Our recent results have shown that mesoporous molecular sieve AlSBA-15 is a more active catalyst for the alkylation reaction compared with HZSM-5, HY, and AlMCM-41, owing to its large pore size and abundant medium-strong acid sites [14]. However, the reusability of AlSBA-15 catalyst for this reaction is very poor because of its relatively low thermal and hydrothermal stability in the reaction and/or the regeneration cycles, and the 2-TBHQ yield drops to about 1/3 after three runs. To improve the reusability of this catalyst, MSU-$S_{(BEA)}$, a new kind of mesoporous molecular sieve with higher thermal stability, has been tried [15,16], but the results remain unsatisfying. The product yield on MSU-$S_{(BEA)}$ is reduced by 8% after three reuses, due to partial dealumination and collapse of the mesostructure of MSU-$S_{(BEA)}$ during the reaction and/or regeneration cycles. Consequently, the continued search for more effective catalysts should focus on materials with more stable structures and greater numbers of accessible acid sites.

MCM-49 was first reported by Mobil researchers in 1993 [17]. The structure of calcined MCM-49 has a topology virtually identical to that of MCM-22 [18]. MCM-49 is formed when

* Corresponding authors. Fax: +86 21 65641740.
E-mail addresses: yhyue@fudan.edu.cn (Y. Yue), zigao@fudan.edu.cn (Z. Gao).

0021-9517/$ – see front matter
doi:10.1016/j.jcat.2006.02.023

the molar ratio of organic template (hexamethyleneimine) and inorganic cations in the synthesis mixture is <2.0. Its framework topology comprises two independent pore systems, one consisting of two-dimensional sinusoidal channels with an effective diameter of 10 member ring and the other consisting of large supercages with an inner diameter of 7.1 Å and a height of 18.2 Å [18–21]. The surface of the platelike crystals is covered with 12 member ring pockets, each of which is half of a supercage with an approximate depth of 7 Å [21]. These opened pockets on the external surface provide easily accessible acid sites and can readily accommodate bulky reaction intermediates; thus the zeolite could be an efficient catalyst for chemical processes involving bulky molecules.

In this work, MCM-49 samples with different Si/Al ratios were prepared. Their textural, structural, and acid properties were characterized by powder X-ray diffraction (XRD), X-ray fluorescence (XRF), ^{27}Al MAS nuclear magnetic resonance (NMR), BET analysis, scanning electron microscopy (SEM), NH_3 and 2,6-di-*tert*-butyl-pyridine (DTBPy) temperature-programmed desorption (TPD), and acid-catalyzed model reactions. The catalytic activity and stability of the samples toward alkylation of hydroquinone with *tert*-butanol were tested and compared with those of ZSM-5 and USY zeolites. The positive role of the external acid sites on MCM-49 in the reaction was proven.

2. Experimental

2.1. Catalyst preparation

MCM-49 with Si/Al ratios of 10, 15, 20, 25, and 30 were prepared following previously described procedures [22]. Typically, 12.0 mL of hexamethyleneimine was added to a solution containing 2.02 g of sodium hydroxide, a calculated amount of sodium aluminate, and 160 mL of deionized water. Then 13.4 g of fumed silica was slowly added to the solution, and the slurry was stirred rigorously for 1 h to form the initial gel. The gel was transferred to a Teflon-lined autoclave heated at 150 °C for 72 h. The white precipitate thus obtained was filtered, dried at 100 °C overnight, and finally calcined in air by heating to 540 °C at a rate of 5 °C/min and maintaining this temperature for 5 h to completely remove the surfactant. The samples were then ion-exchanged with 1 mol/L NH_4NO_3 at 80 °C for 12 h twice and then recalcined at 540 °C for 5 h. The final products are designated as MCM-49(X), where X represents the Si/Al ratio in the reactant gel.

HZSM-5 zeolite with a Si/Al ratio of 23.4 was supplied by Shanghai No. 7 Chemical Dye Factory, and HUSY zeolite with a unit size parameter of 24.44 Å was provided by Fushun Research Institute of Petroleum and Petrochemicals. These are denoted as ZSM-5 and USY, respectively.

Silanized MCM-49(20) catalysts were prepared by adding a certain amount of tetraethyl orthosilicate (TEOS) into the slurry of 1 g of MCM-49(20) and 5 mL of cyclohexane under rigorous stirring. After 30 min, the slurry was dried and finally calcined at 500 °C for 3 h. The TEOS-treated samples are designated as SiMCM-49-*n*, with *n* representing the volume of TEOS added (μL/g).

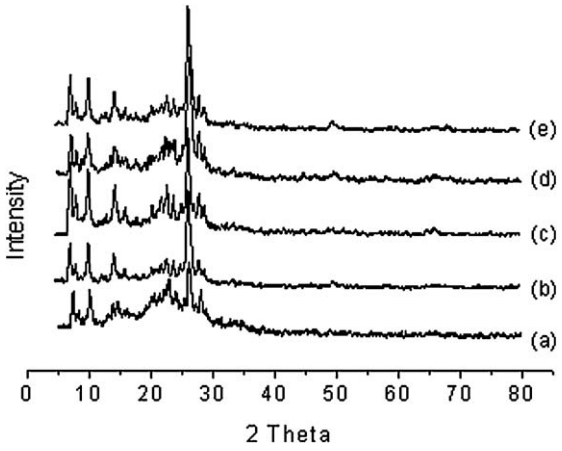

Fig. 1. XRD patterns of calcined MCM-49 catalysts with gel Si/Al ratios of (a) 10; (b) 15; (c) 20; (d) 25; (e) 30.

2.2. Characterization

Powder XRD patterns were recorded on a Bruker D4 ENDEAVOR diffractometer using Cu-K_α radiation at 40 kV and 40 mA with a scan speed of 1°/min. The bulk Si/Al ratio of the zeolites was determined by XRF on a Philips PW2404 elemental analysis spectrometer. The N_2 adsorption/desorption isotherms were measured on a Micromeritics ASAP2000 instrument at liquid N_2 temperature. Specific surface areas were calculated from the adsorption isotherms by the Langmuir method. ^{27}Al MAS NMR spectra were recorded using a Bruker MSL-300 spectrometer, with a resonance frequency of 78.205 MHz, a recycle delay of 0.5 s, short 0.8 μs pulses, a spectral width of 15.625 kHz, and a spin rate of 4 kHz. NH_3 and DTBPy TPD of the samples were carried out in a flow-type fixed-bed reactor at ambient pressure. The catalysts were pretreated at 550 and 650 °C, respectively, for 2 h in He flow. The NH_3/DTBPy adsorption temperature was 120 °C, and the temperature was raised at a rate of 10 °C/min. The NH_3 desorbed was collected in a liquid N_2 trap and detected by gas chromatography, and the DTBPy desorbed was detected by on-line gas chromatography.

2.3. Activity tests

The activities of the samples toward cumene cracking and 1,3,5-tri-*tert*-butyl-benzene (TTBB) dealkylation were tested in a pulse microreactor. The catalyst load for the tests was 10 mg, and the catalyst was preheated at 450 °C for 2 h before reaction. Hydrogen at a flow rate of 60 mL/min was used as the carrier gas. The reactions were conducted at 200 °C, and 1 μL of cumene or 5 μL of a mixture of TTBB and cyclohexane (molar ratio, 1:3) was injected for each test. The products were analyzed by an on-line gas chromatograph equipped with a thermal conductivity detector.

Alkylation of hydroquinone with *tert*-butanol was carried out in an autoclave equipped with a magnetic stirrer. Typically,

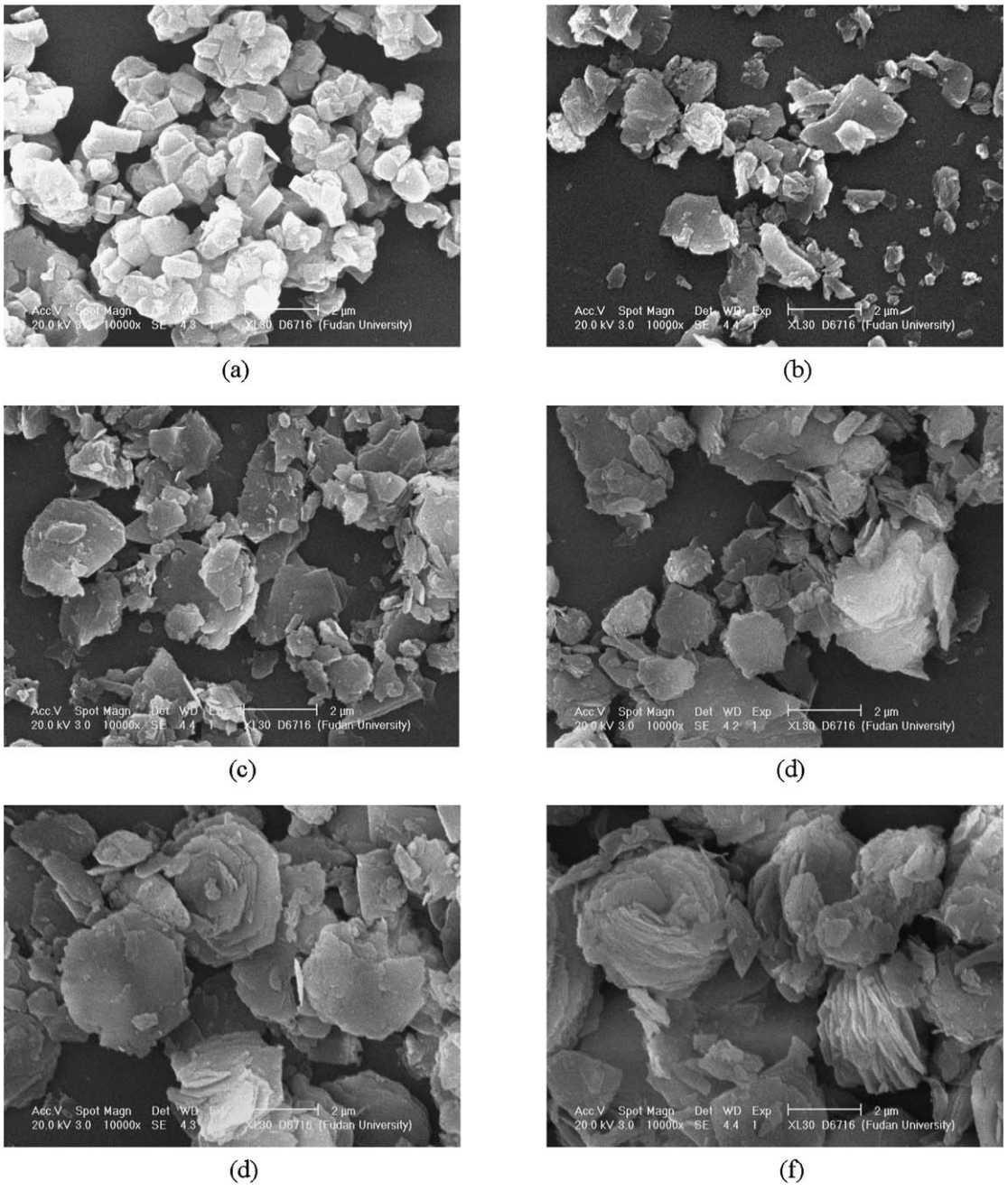

Fig. 2. SEM images of (a) ZSM-5 and MCM-49 catalysts with gel Si/Al ratios of (b) 10; (c) 15; (d) 20; (e) 25; (f) 30.

0.5 g of hydroquinone, 1.0 g of *tert*-butanol, and 0.25 g of catalyst were added to the autoclave, along with 2 g of xylene as a solvent. The reaction lasted about 4 h. The products were analyzed with a gas chromatograph equipped with a SE-54 capillary column (30 m × 0.25 mm × 0.3 μm) and a flame ionization detector.

3. Results and discussion

3.1. Characterization

MCM-49 samples with Si/Al ratios of 10, 15, 20, 25, and 30 were prepared. The XRD patterns of these samples are shown in Fig. 1. The three characteristic peaks of MCM-49 zeolite at about 7.1°, 9.9°, and 26.0° 2θ are observed in the patterns of all samples. The peak intensities are almost the same for all samples except the sample with a Si/Al ratio of 10, indicating that this sample has poorer crystallinity than the other samples.

SEM images of the MCM-49 samples are shown in Fig. 2. All of the MCM-49 samples exhibit platelike crystal morphology, and their average crystal size is larger than that of the ZSM-5 sample. The size and uniformity of the MCM-49 crystals increase with their Si/Al ratios.

The bulk Si/Al ratio of the crystallized MCM-49 catalysts measured by XRF is generally somewhat smaller than that of the initial gel, indicating that Al is probably easier than Si to

Table 1
Composition and textural properties of the catalysts

Catalyst	Gel Si/Al ratio[a]	Bulk Si/Al ratio[b]	Crystal size (μm)[c]	Relative crystal-linity (%)[d]	Pore volume (cm^3/g)	Surface area (m^2/g)
MCM-49(10)	10	10	0.3–3	61	0.15	398
MCM-49(15)	15	13	1–3	89	0.17	406
MCM-49(20)	20	19	1–3	100	0.20	416
MCM-49(25)	25	23	1–3	98	0.18	393
MCM-49(30)	30	28	1–3	98	0.19	409
ZSM-5	–	23[e]	1	–	0.20	470
USY	–	4.3[f]	–	–	0.36	831

[a] Calculated from the amount of fumed silica and sodium aluminate added in the reactant gel.
[b] Determined by XRF.
[c] Estimated from SEM images.
[d] Take MCM-49(20) catalyst as 100% crystallinity.
[e] Calculated from ^{29}Si MAS NMR.
[f] Calculated from the unit size parameter.

incorporate into the framework of MCM-49 during synthesis. The composition and textural properties of the MCM-49 samples are summarized in Table 1. The BET surface areas and pore volumes of the samples are in the range of 393–416 m^2/g and 0.15–0.20 cm^3/g, respectively.

Fig. 3 depicts the ^{27}Al MAS NMR spectra of the samples. An intense line at 55 ppm from four-coordinate aluminum in the zeolite-like framework and a weak line at 0 ppm from extra-framework six-coordinated aluminum are observed. The relative intensity of the extra-framework six-coordinate Al in all of the samples is about 1/4, demonstrating that most of the Al species has been incorporated into the framework of the zeolites.

3.2. Acidity measurement

3.2.1. NH_3 TPD

The acidity of the MCM-49 samples was evaluated by NH_3 TPD. Fig. 4 and Table 2 give the TPD profiles and the data for the samples calculated using a Gaussian fitting program, along with those of ZSM-5 and USY for comparison. There are evidently two peaks on the TPD profiles of all of the samples. The low- and high-temperature peaks at about 258–277 °C and 420–467 °C, respectively, correspond to the weak and strong acid sites of the samples. The total number of acid sites, as well as the number of strong acid sites, of the MCM-49 samples decrease with increasing Si/Al ratio, but nonetheless are much smaller than that of ZSM-5 and USY.

3.2.2. DTBPy TPD

To characterize the external acid sites of MCM-49 samples, DTBPy was used as the base probe in TPD tests. This choice was made because previous study [23] revealed that the large DTBPy molecules adsorbed only on the Brønsted acid sites located on the external surface of zeolitic catalysts with 10-MR and unidirectional 12-MR pore channel systems. Fig. 5 shows the DTBPy-TPD profiles of the MCM-49 samples, and Table 3 summarizes the data. As shown in Fig. 5, all the TPD profiles have three peaks at temperatures of about 240, 330, and 540 °C,

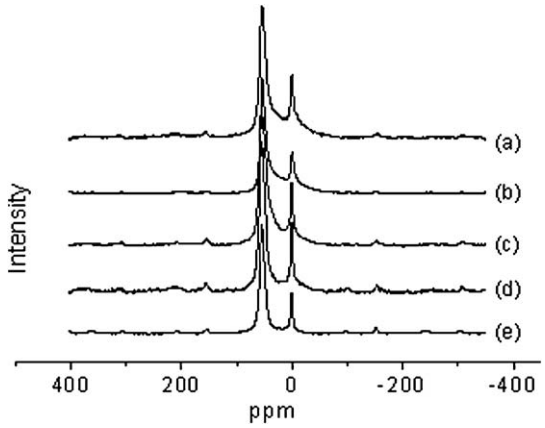

Fig. 3. ^{27}Al MAS NMR spectra of MCM-49 catalysts with gel Si/Al ratios of (a) 10; (b) 15; (c) 20; (d) 25; (e) 30.

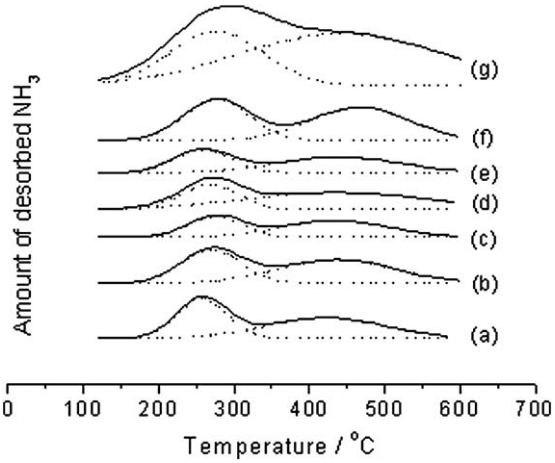

Fig. 4. NH_3-TPD curves of MCM-49 with gel Si/Al ratios of (a) 10; (b) 15; (c) 20; (d) 25; (e) 30; (f) ZSM-5; (g) USY.

Table 2
NH_3-TPD data of various catalysts

Catalyst	Peak temperature (°C)		Amount of desorbed NH_3 (mmol/g)		
	I	II	I (120–350 °C)	II (350–600 °C)	Total
MCM-49(10)	258	420	0.28	0.31	0.59
MCM-49(15)	273	429	0.21	0.28	0.49
MCM-49(20)	274	433	0.21	0.25	0.46
MCM-49(25)	270	435	0.16	0.21	0.37
MCM-49(30)	261	437	0.15	0.18	0.33
ZSM-5	277	467	0.25	0.50	0.75
USY	271	421	0.84	1.0	1.8

respectively. The results for the three different types of zeolites are compared in Fig. 6 and Table 3. The percentages of external acid sites are much higher on the MCM-49 samples than on ZSM-5; in particular, the number of strongest acid sites is two to three times greater on the former than on the latter. The pockets on the external surface of MCM-49 may account for the excessive external acid sites, whereas trapping of the probe molecules in the hemispheric pockets is responsible for the increased desorption temperature on TPD profiles. The external acid site percentage is evidently greater on USY zeolite than

Table 3
DTBPy-TPD data of the catalysts

Catalyst	Peak temperature (°C)			Amount of desorbed DTBPy (μmol/g)				External acid site[a] (%)
	I	II	III	I (120–300 °C)	II (300–500 °C)	III (500–700 °C)	Total	
MCM-49(10)	243	323	513	34	12	5	51	8.6
MCM-49(15)	236	320	516	25	11	7	43	8.8
MCM-49(20)	240	337	564	23	10	10	43	9.3
MCM-49(25)	237	328	551	20	10	9	39	11
MCM-49(30)	251	329	524	17	11	6	34	10
ZSM-5	233	373	–	23	19	3	45	6.0
USY	295	–	580	30	91	190	310	17

[a] Calculated by the following equation: external acid site (%) = (total amount of external acid site (from DTBPy-TPD))/(total amount of acid site (from NH_3-TPD)) × 100%.

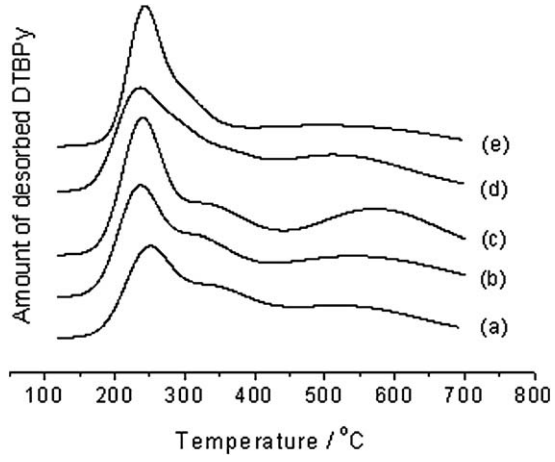

Fig. 5. DTBPy-TPD curves of MCM-49 with Si/Al ratios of (a) 10; (b) 15; (c) 20; (d) 25; (e) 30.

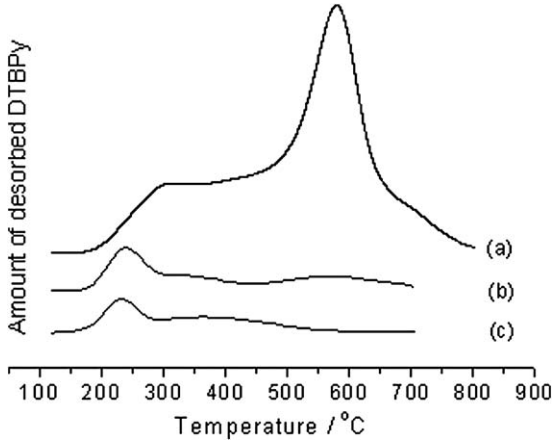

Fig. 6. DTBPy-TPD curves of (a) USY; (b) MCM-49(20); (c) ZSM-5.

on the other two zeolites, due to the tridirectional 12-MR and the secondary pore system in the structure of the former. Because the external acid sites on the opened pockets are more accessible to bulky molecules than the acid sites within the microporous framework of the zeolites, the abundance of pocket acid sites for MCM-49 zeolite and the stronger adsorption of reactant molecules on these sites should be advantageous when the zeolite is used as catalyst for acid-catalyzed reactions of bulky molecules.

Table 4
Catalytic activities for cumene cracking and TTBB dealkylation at 200 °C

Catalyst	Conversion of cumene (%)	Conversion of TTBB (%)	Selectivity (%)		
			Benzene	TBB[a]	DTBB[b]
MCM-49(10)	4	43	18	29	53
MCM-49(15)	4	57	30	31	39
MCM-49(20)	5	76	42	27	31
MCM-49(25)	5	71	39	30	31
MCM-49(30)	5	54	30	31	39
ZSM-5	30	5.6	0	0	100
USY	84	100	86	14	0

[a] Represents *tert*-butyl-benzene.
[b] Represents di-*tert*-butyl-benzene.

3.3. Model reaction tests

3.3.1. Cracking of cumene

Cumene cracking is a typical strong acid-catalyzed reaction. The catalytic activities of the MCM-49 samples for this reaction were tested and compared with those of ZSM-5 and USY. The results, given in Table 4, show that the MCM-49 samples have much lower activities than ZSM-5 and USY. This finding correlates quite well with the NH_3 TPD results indicating that MCM-49 has a much lower number of strong acid sites than ZSM-5 and USY, because all of the acid sites on these zeolites are accessible to the relatively small cumene molecules.

3.3.2. Dealkylation of TTBB

The dealkylation of TTBB (with a molecular dimension of 0.94 nm) was chosen as a model acid-catalyzed reaction of bulky molecules. The reaction data for the samples are also given in Table 4. As expected, the activities of the MCM-49 samples become much higher than that of ZSM-5, showing that in this case the external strong acid sites on MCM-49 play an important role, because the large TTBB molecules have difficulty entering the 12-MR and 10-MR pore systems of the zeolites. Unlike ZSM-5, the USY zeolite catalyst remains very active for the dealkylation reaction, demonstrating that some of the strong acid sites on USY are accessible to TTBB molecules. This finding is in agreement with the results of DTBPy TPD measurement.

It is interesting to note the marked difference in the product distribution of the zeolites. The selectivities to benzene, TBB, and DTB are almost even on MCM-49, whereas DTBB is the

Table 5
Reaction data of alkylation of hydroquinone on the catalysts

Catalyst	Reaction temp. (°C)	Conversion (%)	Selectivity (%)		2-TBHQ yield (%)
			2-TBHQ	2,5-DTBHQ	
MCM-49(10)	150	38	76	24	29
MCM-49(15)	150	53	73	27	39
MCM-49(20)	150	65	70	30	46
MCM-49(25)	150	63	71	29	45
MCM-49(30)	150	46	74	26	34
MCM-49(20)	130	43	79	21	34
MCM-49(20)	140	50	78	22	39
MCM-49(20)	160	67	67	33	45
MCM-49(20)	170	71	54	46	38
ZSM-5	150	20	97	3	19
USY	150	48	85	15	41

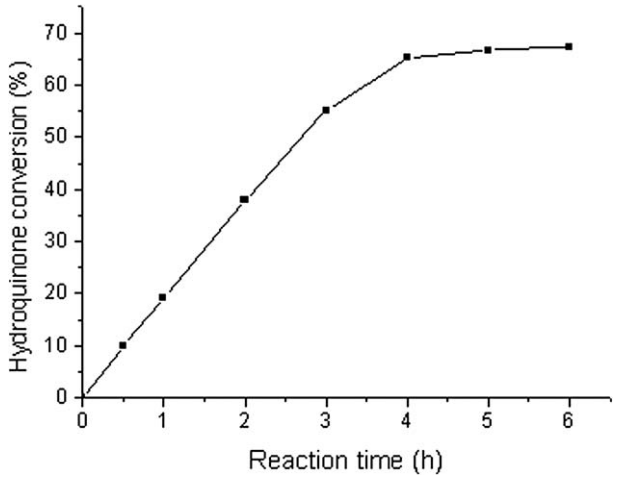

Fig. 7. Conversion of hydroquinone over MCM-49(20) as a function of reaction time at 150 °C.

sole reaction product on ZSM-5 and benzene is the major product on USY. It seems that complete dealkylation is favored with increasing depth of penetration of the reactant molecules into the zeolite pore system. This suggests that the likelihood of further dealkylation of the reaction intermediates is enhanced due to the prolonged residence of these intermediates on the catalyst surface.

3.4. Alkylation of hydroquinone on MCM-49 catalysts

The activities of MCM-49 and other zeolite samples for alkylation of hydroquinone were investigated; the results are summarized in Table 5. During reaction, only 2-*tert*-butylhydroquinone (2-TBHQ) and 2,5-di-*tert*-butyl-hydroquinone (2,5-DTBHQ) were found in the products. No other byproducts, such as ether or paraffin, were formed under all conditions. The alkylation of hydroquinone on the catalysts at 150 °C reached equilibrium after around 4 h, as shown in Fig. 7, and the reaction data in the discussions that follow were taken after 4 h on stream for comparison purposes.

The catalytic behavior of the MCM-49 samples changes with changes in their Si/Al ratios. The alkylation activity of the catalysts is in the order of MCM-49(20) > MCM-49(25) > MCM-49(15) > MCM-49(30) > MCM-49(10). The catalysts' selectivity to 2-TBHQ is slightly decreased as the activity is increased. The order of the alkylation activity parallels that for the TTBB dealkylation activity, indicating that the external strong acid sites are probably the main active sites for both reactions. The ZSM-5 and USY catalysts are less active than the MCM-49(20) catalyst. The difference in activities of the USY catalyst for the liquid-phase alkylation of hydroquinone and the gas-phase dealkylation of TTBB may arise from the significant increase in diffusion resistance in liquid phase reaction, along with the different kinetics and mechanisms of these two reactions. This merits further study, however.

Table 6
DTBPy-TPD data of TEOS treated MCM-49(20) catalysts

Catalyst	Peak temperature (°C)			Amount of desorbed DTBPy (μmol/g)			
	I	II	III	I (120–300 °C)	II (300–500 °C)	III (500–700 °C)	Total
MCM-49(20)	240	337	564	23	10	10	43
SiMCM-49-20	240	335	547	20	9	9	38
SiMCM-49-100	240	323	536	19	8	6	33
SiMCM-49-150	237	317	520	19	8	4	31
SiMCM-49-200	249	324	518	19	6	3	28
SiMCM-49-400	248	325	507	17	4	1	22

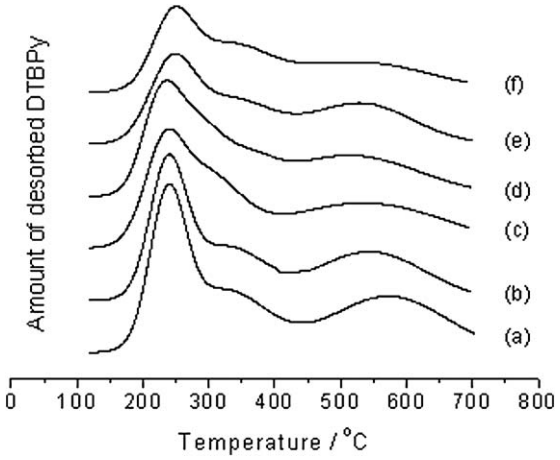

Fig. 8. DTBPy-TPD curves of (a) MCM-49(20); (b) SiMCM-49-20; (c) SiMCM-49-100; (d) SiMCM-49-150; (e) SiMCM-49-200; (f) SiMCM-49-400.

The effect of reaction temperature on the alkylation of hydroquinone on the MCM-49 samples was also studied; the results are given in Table 5. Increased hydroquinone conversion and decreased 2-TBHQ selectivity were observed with increasing reaction temperature, similar to the results obtained over AlSBA-15 [14] and MSU-$S_{(BEA)}$ [15]. An optimum 2-TBHQ yield of 46% was obtained over the MCM-49(20) catalyst at a reaction temperature of 150 °C, which is close to the results for the mesoporous catalysts [14,15].

To confirm the role of the external acid sites in the alkylation reaction, the MCM-49(20) catalyst was treated with various amounts of TEOS using a chemical liquid deposition method to allow the external acid sites to be covered with silica to some extent [24–26]. DTBPy-TPD profiles of the TEOS-treated

Table 7
Reaction data of the TEOS treated MCM-49(20) catalysts

Catalyst	Reaction temp. (°C)	Conversion (%)	Selectivity (%)		2-TBHQ yield (%)
			2-TBHQ	2,5-DTBHQ	
MCM-49(20)	150	65	70	30	46
SiMCM-49-20	150	60	72	28	43
SiMCM-49-100	150	31	80	20	25
SiMCM-49-150	150	23	84	16	19
SiMCM-49-200	150	16	92	8	15
SiMCM-49-400	150	6	93	7	6

Table 8
Comparison of reusability of catalysts

Catalyst	Cycle	Reaction temp. (°C)	Conversion (%)	Selectivity (%)		2-TBHQ yield (%)
				2-TBHQ	2,5-DTBHQ	
MCM-49(20)	1	150	65	70	30	46
MCM-49(20)	2	150	63	71	29	45
MCM-49(20)	3	150	64	73	27	47
USY	1	150	48	85	15	41
USY	2	150	46	85	15	39
USY	3	150	46	86	14	40
AlSBA-15 [14]	1	150	65	81	19	53
AlSBA-15 [14]	2	150	29	100	0	29
AlSBA-15 [14]	3	150	18	100	0	18
MSU-$S_{(BEA)}$ [15]	1	150	76	72	28	55
MSU-$S_{(BEA)}$ [15]	2	150	67	78	22	52
MSU-$S_{(BEA)}$ [15]	3	150	63	81	19	51

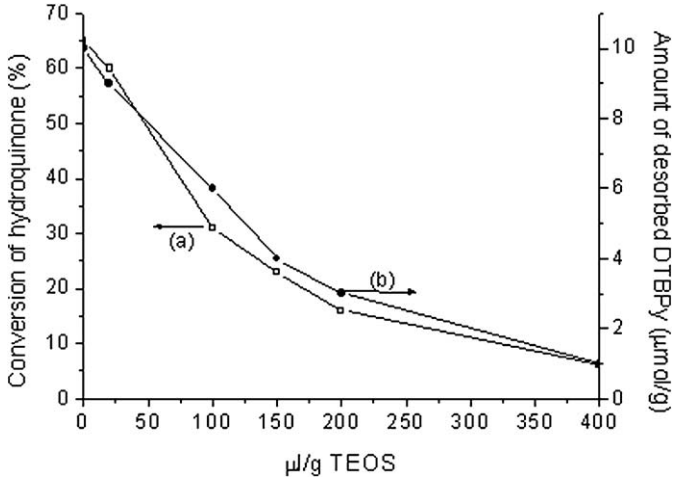

Fig. 9. Effect of TEOS treatment on MCM-49(20) catalysts. (a) The conversion of hydroquinone versus the amount of TEOS (□); (b) The amount of DTBPy desorbed at above 500 °C versus the amount of TEOS (●).

MCM-49(20) samples are given in Fig. 8 and Table 6. As the amount of TEOS increased, the total amount of external acid sites decreased, particularly the amount of strong acid sites. Hence, the peak temperature of the strong acid sites decreased gradually with increased addition of TEOS.

Table 7 gives the reaction data of the TEOS-treated MCM-49(20) catalysts. The alkylation activity of the catalysts decreased considerably as the degree of poisoning by TEOS is

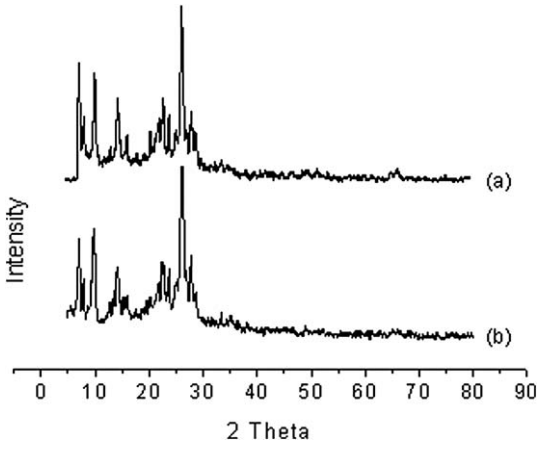

Fig. 10. XRD patterns of (a) fresh MCM-49(20); (b) reused MCM-49(20) (3 cycles).

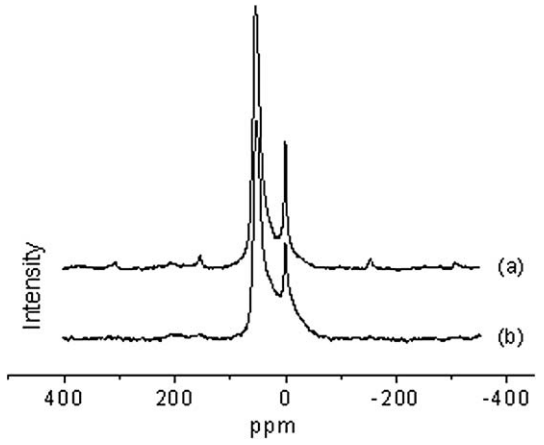

Fig. 11. ^{27}Al MAS NMR spectra of (a) fresh MCM-49(20); (b) reused MCM-49(20) (3 cycles).

increased. The reduction in activity correlates very well with the decreased amount of external strong acid sites on the catalysts as shown in Fig. 9.

3.5. Reusability of MCM-49 catalyst

The reusability of MCM-49(20) and USY catalysts was also studied. After reaction, the catalysts were filtered, washed with ethanol three times, calcined in air at 500 °C for 3 h, and then reused in the reaction. The reaction data, along with some literature data for comparison, are given in Table 8.

The zeolite-type catalysts MCM-49(20) and USY are obviously more stable than the mesoporous molecule sieve catalysts AlSBA-15 and MSU-$S_{(BEA)}$. Catalyst stability decreases in the order of MCM-49(20) ≈ USY > MSU-$S_{(BEA)}$ > AlSBA-15. The crystalline zeolite framework of MCM-49(20) and USY is more resistant to thermal and hydrothermal treatments than the amorphous framework of the mesoporous materials. XRD patterns of the fresh and reused MCM-49(20) catalyst shown in Fig. 10 indicate that the crystalline structure of MCM-49(20) remains intact after reaction and regeneration.

Table 9
Properties of fresh and reused MCM-49(20) catalysts

Catalyst	Al_{EXF}/Al_F	Relative crystallinity (%)	Pore volume (cm^3/g)	Surface area (m^2/g)
MCM-49(20) (fresh)	0.26	100	0.20	416
MCM-49(20) (3 cycles)	0.28	99	0.19	407

^{27}Al MAS NMR spectra of the fresh and reused (for three cycles) MCM-49(20) catalysts in Fig. 11 appear similar. Both have two sharp peaks situated at about 0 and 55 ppm, corresponding to the extra-framework and framework aluminum species in the zeolite. The Al_{EXF}/Al_F ratios calculated from the intensities of the two peaks are given in Table 9, indicating that dealumination of the zeolite during reaction and regeneration can be neglected. Table 9 also compares the textural properties of the fresh and reused catalysts. Only a very slight decrease in specific surface area and pore volume of the catalyst after reuse is observed.

4. Conclusion

MCM-49 zeolite was found to be an ideal catalyst for liquid-phase acid-catalyzed reactions of bulky molecules. Both higher activity and higher stability were obtained for the alkylation of hydroquinone with *tert*-butanol over MCM-49 compared with ZSM-5, USY, AlSBA-15, and MSU-$S_{(BEA)}$ catalysts. The conversion of hydroquinone and the yield of 2-TBHQ at 150 °C were 65 and 46%, respectively. No decrease in the yield of 2-TBHQ was observed after three reaction cycles. Careful acidity measurements by DTBPy-TPD and model acid-catalyzed reaction tests of TTBB dealkylation proved that the high activity derives from the abundance of strong acid sites on the external surface pockets of the zeolite structure. Meanwhile, the high stability can be attributed to the crystalline zeolite framework of MCM-49, which is more thermally and hydrothermally stable than the amorphous framework of the mesoporous molecular sieves.

Acknowledgments

This work was supported by the Chinese Major State Basic Research Development Program (grant 2000077507) and the Shanghai Major Basic Research Program (grant 03DJ14004).

References

[1] J. Kroupa, J. Podstata, V. Matous, Czech Patent 265,262 (1990).
[2] H. Nakamura, JP Patent 6,281,342 (1987).
[3] H. Nakamura, JP Patent 6,281,341 (1987).
[4] M. Hojo, J. Org. Chem. 49 (1984) 4161.
[5] T. Fujita, K. Takahata, JP Patent 03,169,832 (1991).
[6] C. Young, D.B. Campbell, Ind. Eng. Chem. Res. 24 (1990) 642.
[7] G.D. Yadav, N. Kirthivasan, J. Chem. Soc., Chem. Commun. (1995) 203.
[8] G.D. Yadav, V.V. Bokade, Appl. Catal. A 147 (1996) 299.
[9] G.D. Yadav, N. Kirthivasan, Appl. Catal. A 154 (1997) 29.
[10] G.D. Yadav, N.S. Doshi, Catal. Today 60 (2000) 263.
[11] G.D. Yadav, A.A. Pujari, A.V. Joshi, Green Chem. 1 (1999) 269.
[12] P. Selvam, S.E. Dapurkar, Catal. Today 96 (2004) 135.
[13] A. Vinn, M. Karthik, M. Miyahara, V. Murrgesan, K. Ariga, J. Mol. Catal. A 230 (2005) 151.
[14] B.J. Xu, W.M. Hua, Y.H. Yue, Y. Tang, Z. Gao, Catal. Lett. 100 (2005) 95.
[15] B.J. Xu, H.Y. Li, W.M. Hua, Y.H. Yue, Z. Gao, Microporous Mesoporous Mater. 88 (2006) 191.
[16] Y. Liu, W.Z. Zhang, T.J. Pinnavaia, Angew. Chem. Int. Ed. Engl. 40 (2001) 1255.
[17] J.M. Bennett, C.D. Chang, S.L. Lawton, M.E. Leonowicz, D.N. Lissy, M.K. Rubin, US Patent 5,236,575 (1993).
[18] S.L. Lawton, A.S. Fung, G.J. Kennedy, L.B. Alemany, C.D. Chang, G.H. Hatzikos, D.N. Lissy, M.K. Rubin, H.C. Timken, S. Steuernagel, D.E. Woessner, J. Phys. Chem. 100 (1996) 3788.
[19] G.J. Kennedya, S.L. Lawtona, A.S. Funga, M.K. Rubina, S. Steuernagel, Catal. Today 49 (1999) 385.
[20] A.L.S. Marques, J.L.F. Monteiro, H.O. Pastore, Microporous Mesoporous Mater. 32 (1999) 131.
[21] S.L. Lawton, M.E. Leonowicz, R.D. Partridge, P. Chu, M.K. Rubin, Microporous Mesoporous Mater. 23 (1998) 109.
[22] Y.C. Shang, W.X. Zhang, T. Li, T.H. Wu, Chin. J. Catal. 25 (2004) 158.
[23] A. Corma, V. Fornes, L. Forni, F. Marquez, J. Martinez-Triguero, D. Moscottiy, J. Catal. 179 (1998) 451.
[24] Y.H. Yue, Y. Tang, Y. Liu, Z. Gao, Ind. Eng. Chem. Res. 35 (1996) 430.
[25] R.W. Weber, K.P. Moller, M. Unger, C.T. O'Connor, Microporous Mesoporous Mater. 23 (1998) 179.
[26] R.W. Weber, K.P. Moller, C.T. O'Connor, Microporous Mesoporous Mater. 35–36 (2000) 533.